

CHEMISTRY

A European Journal



Accepted Article

Title: Metal-free Halogen(I) Catalysts for Oxidation of (Aryl)(heteroaryl)-methanes to Ketones or Esters : Selectivity Control by Halogen Bond

Authors: SOMRAJ GUHA and Govindasamy Sekar

This manuscript has been accepted after peer review and appears as an Accepted Article online prior to editing, proofing, and formal publication of the final Version of Record (VoR). This work is currently citable by using the Digital Object Identifier (DOI) given below. The VoR will be published online in Early View as soon as possible and may be different to this Accepted Article as a result of editing. Readers should obtain the VoR from the journal website shown below when it is published to ensure accuracy of information. The authors are responsible for the content of this Accepted Article.

To be cited as: *Chem. Eur. J.* 10.1002/chem.201801717

Link to VoR: <http://dx.doi.org/10.1002/chem.201801717>

Supported by
ACES

WILEY-VCH

Metal-free Halogen(I) Catalysts for Oxidation of (Aryl)(heteroaryl)-methanes to Ketones or Esters : Selectivity Control by Halogen Bond

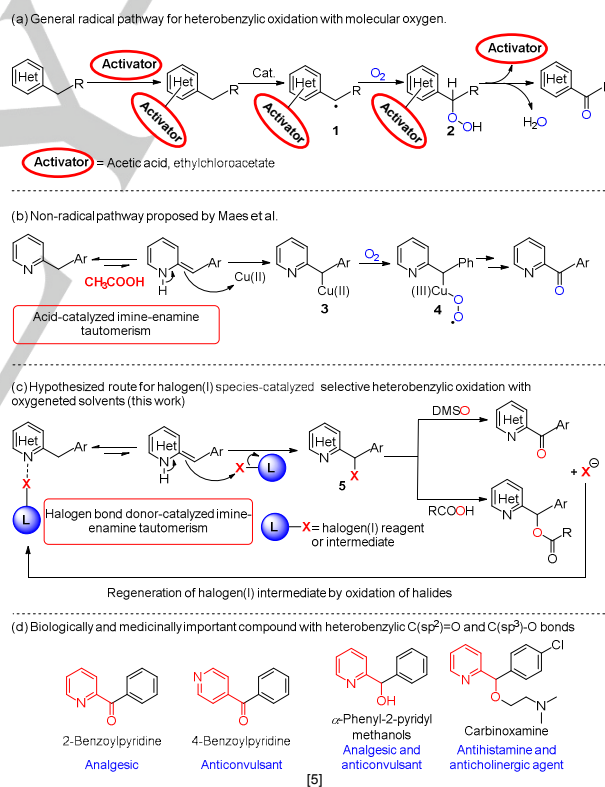
Somraj Guha,^[a] and Govindasamy Sekar^{*[a]}

Abstract: Use of metal-free halogen(I) catalysts has been described for the selective oxidation of (aryl)(heteroaryl)methanes (C(sp³)-H) to ketones (C(sp²)=O) or esters (C(sp³)-O). The synthesis of ketone is carried out with catalytic amount of NBS in DMSO solvent. Experimental studies and Density Functional Theory (DFT) calculation supports the formation of halogen bond (XB) between the heteroarene and NBS which enables imine-enamine tautomerism of the substrates. No additional activator is required for this crucial step. The isotope labelling and other supporting experiments suggest that a Kornblum type oxidation with DMSO and an aerobic oxygenation with molecular oxygen take place simultaneously. A background XB assisted electron transfer (ET) between heteroarenes and halogen(I) catalysts is responsible for the formation of heterobenzylic radical and thus the aerobic oxygenation. For selective acyloxylation (ester formation), catalytic amount of iodine is employed with TBHP in aliphatic carboxylic acid solvent. Several control reactions, spectroscopic study and TD-DFT calculations establish the presence of acetyl hypoiodite as an active halogen(I) species in acetoxylation process. With the help of a selectivity study, for the first time we report that the strength of the XB interaction and the frontier orbital mixing between the substrates and acyl hypoiodites determine the extent of background ET process and thus the selectivity of the reaction.

Halogen-based reagents are employed as efficient organocatalysts and play important roles in developing transition metal-free organic reactions.^[1] Recently, the applications of halogen-bonding (XB), an attractive noncovalent interaction between the electrophilic region (σ -hole) of a substituted halogen atom and a Lewis base, has been successfully introduced in organic synthesis.^[2] In spite of its unorthodox nature,^[2a] this halogen-bonding interaction is already reported as a competent tool for activation of functional group,^[3] photoactivation of halides to generate radical intermediates,^[4] synthesis of recyclable catalysts,^[5] and transformation of gaseous compounds to easily-handled condensed-phase liquid reagents.^[6]

The application of halogen bond in organic synthesis is still in its nascent stage. Importantly, the role of halogen-bonding interaction in controlling the reactivity of halogen based reagents (such as influence of ligands on the reactivity of transition metal

salts^[7] during a reaction is still unexplored. A well-thought-out research on this topic can make the halogen-based reagents a more versatile metal-free alternative. This possibility prompted us to investigate how the easily available electrophilic halogen(I) reagents can act as halogen bond donor catalysts,^[8] and how halogen-bonding interaction can influence the reactivity of the halogen(I) reagents and in situ-generated halogen(I) intermediates.^[9] As a part of this ongoing research, herein, we report a transition metal-free selective oxidation of (aryl)(heteroaryl)methanes (C(sp³)-H) to ketones (C(sp²)=O) or esters (C(sp³)-O) and the vital role of halogen bond in maintaining the selectivity of these processes (Scheme 1).



Scheme 1. General mechanistic approaches for the oxidation of heterobenzylic C(sp³)-H bond and importance of the heterobenzylic C(sp²)=O and C(sp³)-O bonds containing products.

The selective oxidation of heterobenzylic C(sp³)-H bonds to C(sp²)=O or C(sp³)-O bonds are useful and straightforward

[a] Somraj Guha, Prof. G. Sekar
Department of Chemistry, Indian Institute of Technology Madras
Chennai 600036, India
E-mail: gsekar@iitm.ac.in; url: http://chem.iitm.ac.in/faculty/sekar/

methods to obtain heterobenzyl ketones or alcohols (or their protected form, esters) respectively. So far, most of the reported procedures for direct heterobenzyl oxidation describe the formation of only C(sp²)=O bond (ketone) and not the C(sp³)–O bond (alcohols or esters) at the heterobenzyl position.^[10] In fact, to the best of our knowledge, there are no reports available on the selective partial oxidation of heterobenzyl C(sp³)–H bonds to alcohols and very few reports are available on the selective acetoxylation at heterobenzyl position.^[11] Moreover, these heterobenzyl acetoxylation require substrate preactivation by N–oxide formation^[11c–e] or excess amount of transition metals under high pressure of oxygen.^[11a, 11b]

There are two major facts behind the difficulties in selective oxidation of heterobenzyl C(sp³)–H bonds to C(sp³)–O bonds. Firstly, most of the reported oxidation procedures follow a radical pathway where the heterobenzyl radical **1** is formed as an intermediate and molecular oxygen is the sole oxidant (Scheme 1(a)). This highly reactive benzylic radical **1** immediately reacts with molecular oxygen to form peroxy intermediate **2** which converts to ketone via elimination of water. Secondly, if some alcohols are formed by the cleavage of O–O bonds in **2**, they get further oxidized to ketones due to the presence of radical species in the reaction mixture. However, Maes et al. reported an alternative pathway that excludes the formation of heterobenzyl radicals for the selective oxidation of heterobenzyl C(sp³)–H to ketones.^[10g] In this case, stoichiometric amount of acetic acid activates the pyridine ring and enables an imine–enamine tautomerism in the first step. The enamine can attack electrophilic Cu(II) species to form organometallic intermediate **3** followed by **4** and finally the ketone (Scheme 1(b)).^[10d]

In 2008, Bolm et al. reported the halogen–bonding activation of pyridine ring with highly fluorinated bromoalkanes and iodoalkanes.^[12] We envisioned that the electrophilic halogen(I) reagents or intermediates can activate the pyridine ring and enable imine–enamine tautomerism. Furthermore, the enamine can attack the electrophilic halogen(I) center to form **5**, a non–organometallic analogue of **3**. At this point, nucleophilic substitution of halide at benzylic position of **5** with DMSO can lead to the formation of ketone (Kornblum oxidation)^[13] and the same with carboxylic acids (acetic acid) can lead to the formation of esters (acetates), a protected form of alcohols (Scheme 1(c)). For the first time, the oxygenated solvents are utilized as the source of oxygen for this kind of heterobenzyl oxidation. The two independent reactions follow a common mechanistic route and a simple change in solvent helps to obtain two different oxidized products (ketones and esters) selectively. Both of these oxidized products with C(sp²)=O and C(sp³)–O bonds often serve as biologically and medically active compounds (Scheme 1(d)).^[14] Moreover, the number of heteroaromatic ring containing oral drugs is increasing in market.^[15] Presence of pyridine and thiazoles is very common in F.D.A–approved drugs.^[16] Hence, the development of metal–free protocol for the functionalization of heterobenzyl C–H bond is urgent and important to avoid even trace amount of transition metal salt contamination with these compounds.

Results and Discussion

We started our investigations using *N*-bromosuccinimide (NBS) as a halogen(I) source and 2–benzylpyridine **6a** as a model substrate. Our preliminary investigation was to get the proper insight into the nature of interaction between the 2–benzylpyridine and NBS by quantum chemical calculations in vacuum (Figure 1A) and in DMSO solvent (Figure 1B). For comparison, the 2–benzylpyridine/acetic acid and 2–benzylpyridine/triflic acid systems were studied as well. NBS was observed to act as a halogen bond donor (in both vacuum and DMSO). Acetic acid was observed to act as a hydrogen bond donor and not as a Bronsted acid to activate the pyridine ring (in both vacuum and DMSO). On the contrary, triflic acid is more likely to act as a Bronsted acid to form a “close to ionic” intermediate (in both vacuum and DMSO). The XB interaction energy between NBS and 2–benzylpyridine (–36.7 kcal mol^{–1} in vacuum and –24.3 kcal mol^{–1} in DMSO) is very similar to the HB interaction energy between acetic acid and 2–benzylpyridine (–34.4 kcal mol^{–1} in vacuum and –24.4 kcal mol^{–1} in DMSO). On contrary, the interaction energy between triflic acid and 2–benzylpyridine is extremely high (–49.2 kcal mol^{–1} in vacuum and –35.4 kcal mol^{–1} in DMSO).

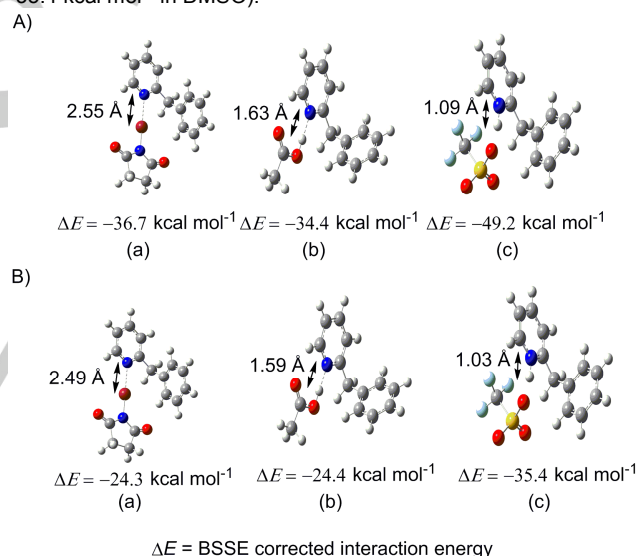


Figure 1. Structure of (a) NBS/2–benzylpyridine (b) acetic acid/2–benzylpyridine and (c) triflic acid/2–benzylpyridine optimized with DFT using M06–2X–D3 functional and 6–311G(d,p) for C,H; 6–311+G(d,p) for N,O; LANL08d basis set in conjunction with the LANL2DZ effective core potential (ECP) for Br in A) vacuum; B) in DMSO (IEFPCM).^[17]

After obtaining information from computational studies, the ¹H NMR shifts of the heterobenzyl protons on interaction of pyridine ring with acetic acid, NBS, and triflic acid were checked (Figure 2). An almost equal downfield shift of the heterobenzyl protons was observed on interaction of pyridine ring with acetic acid ($\delta = 4.14 \text{ ppm}$ to $\delta = 4.17 \text{ ppm}$) and NBS ($\delta = 4.14 \text{ ppm}$ to $\delta = 4.19 \text{ ppm}$). On the other hand, the shift of the heterobenzyl protons was remarkably high ($\delta = 4.14 \text{ ppm}$ to $\delta = 4.34 \text{ ppm}$)

when triflic acid (a strong acid) was allowed to interact with the pyridine ring. These computational and ^1H NMR analyses indicated that NBS can be an appropriate alternative to acetic acid for activation of pyridine ring and can enable the imine–enamine tautomerism.

The formation of halogen bond between NBS and 2–benzylpyridine was further confirmed when the ^1H and ^{13}C NMR spectra of 1:1 mixture of NBS and 2–benzylpyridine was recorded in CDCl_3 (Figure 3). The ^1H NMR peak assigned to the methylenic protons of the succinimide shifted upfield ($\delta = 2.97$ ppm to $\delta = 2.86$ ppm, (Figure 3(a)). The ^{13}C NMR peak of carbonyl carbon of the succinimide moiety shifted downfield ($\delta = 173.2$ ppm to $\delta = 175.2$ ppm, (Figure 3(b)). Both these observations are in accordance with the previous report on halogen–bonded adducts of N–halosuccinimide.^[18] Furthermore, when the spectra of a 1:1:1 mixture of NBS, 2–benzylpyridine and DMSO was recorded in CDCl_3 , more downfield shift was observed for the carbonyl carbon of the succinimide moiety.

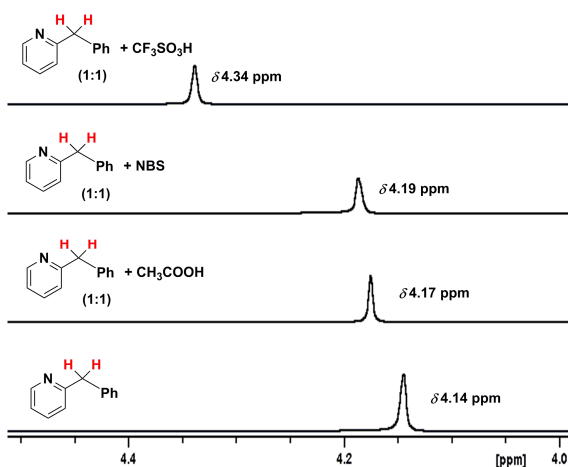


Figure 2. ^1H NMR shifts of the heterobenzyl protons due to interaction of pyridine ring with acetic acid, NBS, and triflic acid in CDCl_3 .

Finally, the ^1H NMR shifts of the heterobenzyl protons on interaction of pyridine ring with acetic acid, NBS, and triflic acid were checked in $\text{DMSO}-d_6$ to verify the presence of XB interaction in a polar solvent such as DMSO. Both the HB interaction between acetic acid with **6a** and the XB interaction between NBS and **6a** was appeared as weak interaction in DMSO (Figure S12, Supporting Information). The binding constant of the XB and HB complexes were calculated with ^1H NMR titration followed by fitting the shifts (1:1 model) in Bindfit.^[17, 19] The binding constant of XB complex between NBS and 2–benzylpyridine $K_a(\text{XB}) = 1.17 \pm 0.04 \text{ M}^{-1}$ and the binding constant of HB complexation between acetic acid and 2–benzylpyridine $K_a(\text{HB}) = 0.03 \pm 0.001 \text{ M}^{-1}$. However, this observation established that NBS can interact with **6a** more effectively than with acetic acid in DMSO solvent. As the previous reports already established that acetic acid can enable

imine–enamine tautomerism of **6a**,^[10d, 10g] thus, NBS should enable the imine–enamine tautomerism of **6a** too.

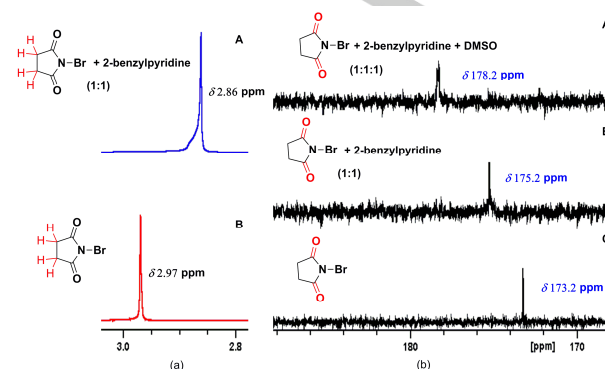


Figure 3. (a) ^1H NMR shifts assigned to the methylenic protons of the succinimide and (b) ^{13}C NMR shifts of carbonyl carbon of the succinimide on interaction of pyridine ring with acetic acid, NBS, and triflic acid in CDCl_3 .

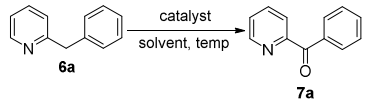
After confirming that NBS can enable an imine–enamine tautomerism by the halogen–bonding activation of pyridine, the oxidation of 2–benzylpyridine (1 mmol) **6a** was tried with stoichiometric amount of NBS (1 equiv) in of DMSO (2 mL) at 100°C . Halogen bonds are weak non–covalent interactions. However, a number of reports are available where halogen–bonding and hydrogen–bonding catalysis occurs at high temperature.^[3d, 20] Gratifyingly, 92% yield of ketone **7a** was isolated after 8 h from the commencement of the reaction (entry 1, Table 1). Use of 1 equivalent of N–iodosuccinimide (NIS) resulted in almost the same yield (90%) after 4 h (entry 2). A large drop in the yield was observed when NIS (30 mol %) was used (entry 3). However, 90 % yield of the ketone was observed with only 30 mol % of NBS after 72 h (entry 4). Bromodimethylsulfonium bromide (BDMS, 30 mol%) also worked efficiently (entry 5) but catalytic iodine was not effective for this reaction (entry 6).

Absence of DMSO in the solvent system completely shut down the reaction (entries 7 and 8) and a 1:1 mixture of DMSO and water provided only 40% yield of the ketone (entry 9). The volume of DMSO could be decreased up to 1 mL (entry 10, 92% yield) but further decrease of solvent volume to 0.5 mL caused a large drop in yield (entry 11, 62% yield). The amount of catalyst could be decreased up to 20 mol % without any noticeable change in reaction rate and product yield (entry 12). To our pleasure, the long reaction time of 72 h could be reduced to 24 h with a slight increase in the reaction temperature to 120°C (entry 13). Decreasing the reaction temperature to 80°C led to a drastic reduction in the yield of the ketone (entry 14).

A complete mechanistic study was performed to probe the reaction pathway. Initially, our priority was to identify the key halogen(I) active species in the reaction mixture. The reaction could be started with either NBS or bromodimethylsulfoxonium ion $[\text{DMSO}-\text{Br}]^+$. It has already been reported by Sudalai et al.

that bromodimethylsulfoxonium ion intermediate is formed due to the interaction of DMSO with NBS.^[21] To prove the formation

Table 1: Optimization of reaction conditions for ketone formation^[a]



entry	catalyst	solvent	temp (°C)	time (h)	yield (%)
1	NBS ^[b]	DMSO	100	8	92
2	NIS ^[b]	DMSO	100	4	90
3	NIS	DMSO	100	72	30 ^[c]
4	NBS	DMSO	100	72	90
5	BDMS	DMSO	100	72	82
6	Iodine	DMSO	100	48	43 ^[c]
7	NBS	toluene	100	48	-
8	NBS	CH ₃ CN	100	48	-
9	NBS	DMSO/water ^[d]	100	48	40
10	NBS	DMSO ^[e]	100	72	92
11	NBS	DMSO ^[f]	100	72	62
12	NBS ^[g]	DMSO ^[e]	100	72	94
13	NBS^[g]	DMSO^[e]	120	24	96
14	NBS ^[g]	DMSO ^[e]	80	48	10

[a] Reaction conditions: **6a** (1 mmol), catalysts (30 mol %), solvent (2 mL); isolated yield, [b] catalyst (1 equiv), [c] 30–35% alcohol phenyl(pyridin-2-yl)methanol was isolated [d] 1:1 ratio of DMSO and water, [e] DMSO (1 mL), [f] DMSO (0.5 mL), [g] NBS (20 mol %)

of this intermediate, Sudalai and co-workers have reported that, two characteristic ¹³C peaks for the carbonyl groups of NBS were observed when equimolar amount of NBS and DMSO were mixed and the ¹³C NMR of the same was recorded in CDCl₃. According to them, one peak was observed at $\delta = 177.8$ ppm (corresponding to free succinimide anion carbonyl peaks) and another was found at $\delta = 179.4$ ppm (corresponding to the DMSO coordinated NBS and showed sufficient downfield shift with respect to free NBS in CDCl₃, $\delta = 173.2$ ppm).^[21]

However, to our surprise, when we recorded the ¹³C NMR spectrum of equimolar amount of NBS and DMSO in presence of equimolar amount of 2-benzylpyridine **6a** in CDCl₃, only one peak at $\delta = 178.2$ ppm was observed (Figure. 3(b), Spectra A). This observation indicated that bromodimethylsulfoxonium ion is not formed in the presence of **6a**. The halogen-bonded complex between NBS and **6a** might be more thermodynamically stable than the complex between NBS and DMSO.

To further prove this hypothesis, the ¹³C NMR spectrum of NBS was recorded in [D₆]DMSO. The characteristic peak of succinimide anions were observed at $\delta = 177.5$ ppm (Figure 4(a), spectrum A). Gratifyingly, when ¹³C NMR spectrum of equimolar mixture of **6a** and NBS was recorded in [D₆]DMSO, the peak at $\delta = 177.5$ ppm disappeared (Figure 4(a), spectrum B). It clearly proved that NBS was not decomposing in DMSO in the presence of **6a**.

Finally, the possible reversible process associated with the interaction between NBS and **6a** (Figure 4(b), Equation 1) and the interaction between NBS and DMSO (Figure 4(b), Equation 2) were thermodynamically quantified. The pK_{eq} ($-\text{Log}K_{eq}$) for these two processes were calculated by DFT.^[17] The self-consistent reaction field (scrf) model was used to account for solvent effects of DMSO. The results showed that the pK_{eq} of reaction (ii) is significantly higher than the pK_{eq} of reaction (i) (Figure 4(b)). The formation of halogen-bonded complex between NBS and **6a** is more thermodynamically favorable than the formation of bromodimethylsulfoxonium ion by dissociation of NBS in DMSO. Hence, the initial reaction started with the interaction of NBS with 2-benzylpyridine.^[22]

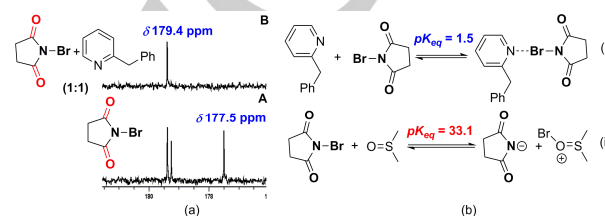


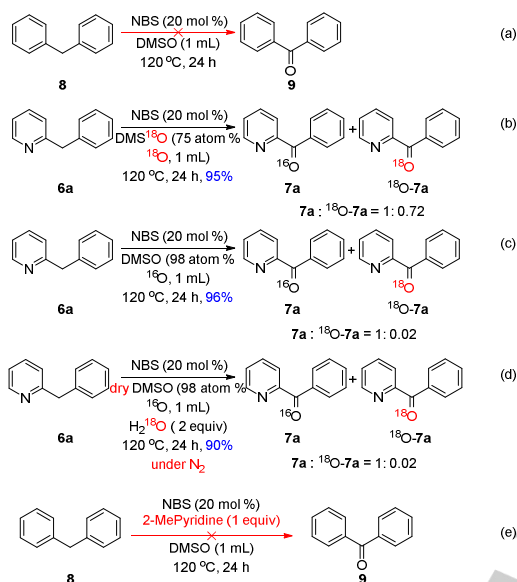
Figure 4. (a) ¹³C NMR spectra of NBS (spectra A) and 1:1 mixture of NBS and 2-benzylpyridine (spectra B) in [D₆]DMSO (b) Calculated pK_{eq} for the formation of halogen-bonded adduct between NBS and **6** [Equation (i)] and the same for the formation of bromodimethylsulfoxonium ion [Equation (ii)] (M06-2X-D3/6-311G(d,p) for C,H; 6-311+G(d,p) for N,O; LANL08d basis set in conjunction with the LANL2DZ effective core potential (ECP) for Br /IEFPCM(DMSO)).^[17]

Several controlled reactions were carried out to predict the complete reaction pathway. First, the diphenylmethane **8** was taken as a starting material to check the importance of the imine/enamine tautomerism in this reaction. No benzophenone **9** was observed after 24 h of the reaction (Scheme 2(a)). This result suggested that the heterobenzylic C–H bonds can be selectively oxidized with this method and that imine–enamine tautomerism is a mandatory step in the pathway.

The reaction was carried out in DMS-¹⁸O (75 atom % ¹⁸O) solvent to find the source of the oxygen in this oxidation process. It was observed that the ¹⁸O-labeled ketone ¹⁸O-**7a** was formed along with ¹⁶O-labeled ketone **7a** with the ratio of 0.72:1 (Scheme 2(b)). However, only 2% of the product was ¹⁸O-labeled ketone ¹⁸O-**7a** when the reaction was carried out in normal DMS-¹⁶O (98 atom % ¹⁶O, Scheme 2(c)). The reaction was also carried out with 2 equiv of H₂¹⁸O in the presence of dry DMS-¹⁶O (98 atom % ¹⁶O). The ¹⁸O-labeled ketone ¹⁸O-**7a** was formed along with ¹⁶O-labeled ketone **7a** with the ratio of 0.02:1 (Scheme 2(d)). These ¹⁸O-labeling experiments suggested that the reaction followed two competitive pathways. In one pathway, the heterobenzylic radical was formed in the reaction mixture and quenched by aerial oxygen. In another pathway, the heterobenzylic bromide was formed which underwent nucleophilic substitution with DMSO (Kornblum oxidation), as per our expectation.

Several radical scavengers were screened at optimized condition for the oxidation of **6a** to **7a** to detect the background

radical pathway.^[17] In presence of TEMPO (1 equiv), the reaction was unaffected (Scheme S5, entry 1, supporting information). However, the yield of the product was decreased to 75% when BHT (1 equiv) was used (Scheme S5, entry 2). The amount of BHT was increased to 2 equiv and the yield of **7a** was decreased up to 60% (Scheme S5, entry 3). It was observed that the yield of **7a** did not decrease further even after increasing the amount of BHT up to 4 equiv (Scheme S5, entry 4, 5).

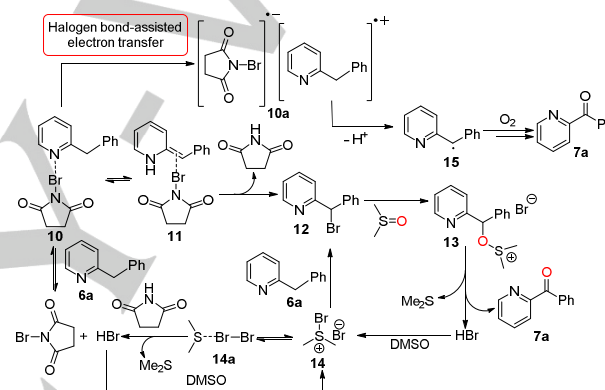


Scheme 2. Controlled experiments to probe the mechanistic pathway

We also tried to find the possible reason behind the formation of heterobenzylic radical as a background reaction. The possibility of thermal decomposition of NBS to generate bromine radical ($\text{Br}\cdot$) followed by the abstraction of heterobenzylic C–H bond to form heterobenzylic radical can be ruled out. This was confirmed when no ketone was formed from diphenylmethane **8** under optimized condition in spite of the negligible difference in homolytic bond dissociation energy (BDE) of benzylic C–H of **8** (326 kJ mole^{-1}) and **6a** (320 kJ mole^{-1}) (Scheme 2(a)).^[10d] Furthermore, when **8** was subjected to oxidation under the standard conditions in the presence of 2-MePyridine (which resembled 2-benzylpyridine and can act as a XB acceptor), ketone **9** was not formed (Scheme 2e). Hence, it was hypothesized that a halogen bond assisted electron transfer process might be the reason behind the formation of the heterobenzylic radical. Roshokha and coworkers reported that halogen bonds can result in a significant lowering of the activation barrier for the electron transfer (ET) from the XB acceptor to XB donor.^[23] The electron transfer from **6a** to NBS could generate the radical cation of **6a** which successively transformed to the heterobenzylic radical.

Based on the supporting experiments and the controlled reactions, the mechanistic pathway has been proposed for this reaction (Scheme 3). The halogen bond between the NBS and

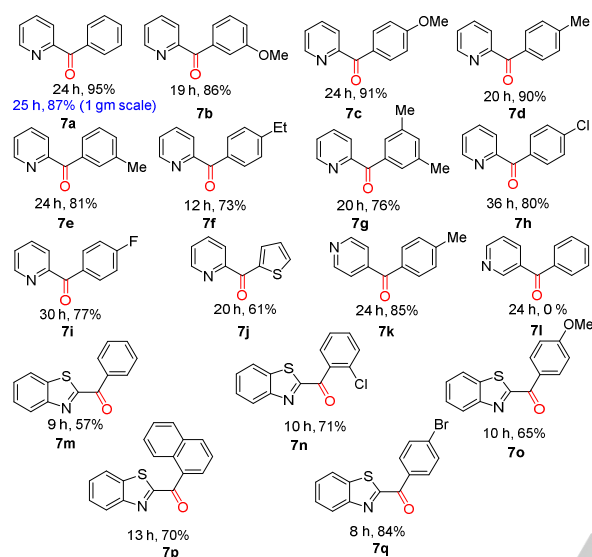
2-benzylpyridine enables the imine–enamine tautomerism. This tautomerism can be represented with the structures **10** and **11**. The enamine attacks NBS to form the heterobenzylic bromide **12**. The heterobenzylic bromide **12** undergoes Kornblum oxidation to form the ketone **7a** via intermediate **13**. The byproduct HBr is immediately oxidized by DMSO to form bromodimethylsulfonium bromide (BDMS) intermediate **14**. This BDMS can act as an alternative halogen(I) source for NBS and can convert the 2-benzylpyridine to heterobenzylic bromide **12** (entry 5, Table 1). Alternatively, this unstable intermediate can be transformed to $[\text{Me}_2\text{S}\rightarrow\text{Br}_2]$ charge–transfer complex **14a** which further reacts with succinimide to regenerate NBS.^[24] The halogen–bonding interaction between NBS and **6a** can also enable a background electron transfer (ET) from **6a** to NBS and the radical ion pair **10a** is generated.^[23b] The radical cation of **6a** can be converted to heterobenzylic radical **15** by eliminating a proton. The ketone **7a** is formed by the quenching of oxygen with **15**.



Scheme 3. Plausible mechanistic pathways for ketone formation

The scope of this metal-free protocol was tested for the benzylic oxidation of a number of heteroarene substrates (Scheme 4). Good to excellent yields of ketones were observed for all the 2-benzylpyridines that contain electron–donating as well as electron–withdrawing arenes (**7b–7i**). When the arene ring is substituted by thiophene ring, yield of the ketone was reduced to 61% (**7j**). Substrate that contained 4–substituted pyridine also provided the corresponding product in good yield (**7k**, 85%). However, substrate that contained 3–substituted pyridine couldn't result in any oxidized product (**7l**). This observation again established the vital role of XB assisted imine–enamine tautomerism of the substrates in this oxidation protocol. Several 2-benzylbenzothiazoles were also found to provide good yield of ketones (**7m–7q**). Substrate with simple benzene ring at heterobenzylic position provided 57% yield of ketone (**7m**). A variety of 2-benzylbenzothiazoles with electron–withdrawing arenes, electron–donating arenes and naphthalene ring present at the heterobenzylic positions were tested and good yields of ketones were obtained (**7n–7q**). Finally, the reaction was tried for a 1 g scale and 87% yield of the ketone was obtained which showed the scalability of the process (entry **7a**).

After the development of NBS catalyzed oxidation of heterobenzylic C(sp³)–H bonds to C(sp²)–O bond, we tried to develop the selective oxidation of heterobenzylic C(sp³)–H bonds to C(sp³)–O bond. The 2-benzylpyridine **6a** was taken as the model substrate and acetic acid was taken as the nucleophilic solvent. However, the mechanistic study for the



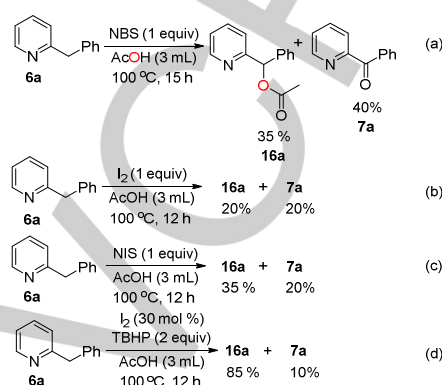
Scheme 4. Substrate scope for the NBS catalyzed hetero-benzylic oxidation.

ketone formation revealed the possibility of a background ET reaction which could lead to the formation of heterobenzylic radical **15** followed by the formation of the ketone **7a** (Scheme 3). As per the assumption, a major problem of selectivity was encountered when NBS (1 equiv) was heated with **6a** (1 equiv) at 100 °C in the presence of acetic acid (3 mL). The reaction was completed within 15 h, but, 35% yield of the acetoxylation product **16a** was isolated along with 40% yield of the ketone **7a** (Scheme 5(a)).

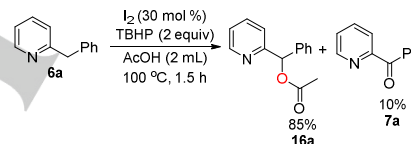
To get better selectivity, several electrophilic iodine sources were checked as catalyst. Only 20% yield of the acetoxylation product was obtained with 20% yield of the ketone when molecular iodine (1 equiv) was employed (Scheme 5(b)). Better selectivity for the formation of acetoxylation product **16a** over the ketone **7a** was observed when more electrophilic iodine sources such as NIS was employed as a halogen(I) source (Scheme 5(c)). However, the yield of acetoxylation product **7a** couldn't be raised.

Next, we thought to employ the in situ-generated hypoiodites as active species. The in situ-generated inorganic hypoiodites and iodates are well known metal-free alternative for oxidative coupling reactions.^[25] These electrophilic hypervalent iodines are unstable but can be generated in situ by the reaction of iodides or iodine with peroxides.^[26] Gratifyingly, 85% yield of **16a** was obtained with only 10% of **7a** within 1.5 h of the commencement of the reaction when **6a** was treated with iodine (precatalyst, 30 mol %) in the presence of

tert-butylhydroperoxide (TBHP, 5–6 (M) in decane, 2 equiv) (Scheme 5(d)). A quick optimization of reaction conditions^[17] revealed that only iodine (30 mol %) is required along with TBHP (2 equiv, 5–6 (M) in decane) and AcOH (2 mL) at 100 °C to complete the reaction in 1.5 h with 85% yield of acetoxylation product (Scheme 6).



Scheme 5. Preliminary screening of conditions to increase the selectivity of the acetoxylation of **6a**



Scheme 6. Optimized reaction conditions for acetoxylation of **6a**

The high selectivity of this process prompted us to go through a detailed mechanistic investigation and to find the key factor that controlled the selectivity of acetoxylation over the ketone formation. Few controlled experiments were designed to find the key intermediate of this oxidation protocol. When the reaction was carried out without the iodine precatalyst, neither acetoxylation nor the ketone formation was observed after 3 h from the commencement of the reaction (Figure 5A, Equation (i)). The presence of the radical trapper TEMPO enhanced the rate of the reaction and the yield of the product was not reduced (Figure 5A, Equation (ii)). This indicated the possibility of a non-radical pathway and the formation of non-radical intermediates in the reaction.

Iodine can be converted to hypoiodous acid (HOI) or hypoiodites (IO[•]) in the presence of peroxides.^[26a, 26c-f] According to the previous reports, hypoiodous acid can be converted to transient acetyl hypoiodite (CH₃COOI) in the presence of acetic acid.^[26b, 27] Acetyl hypoiodite is a well-known electrophilic iodine(I) source which cannot be isolated from the reaction mixture but can be generated in situ and can be used for the stereoselective dihydroxylation of olefins,^[28] iodination of aromatic compounds,^[29] cleavage of vicinal diols,^[30] and oxidation of alcohols.^[9a, 31] We envisaged that acetyl hypoiodite

might be the active halogen(I) intermediate in this acetoxylation reaction.

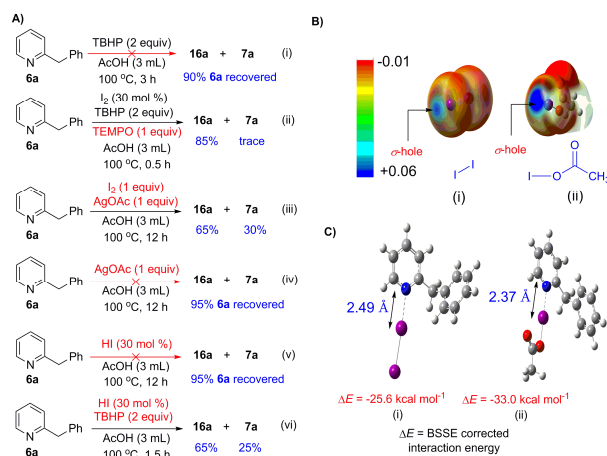


Figure 5. A) Controlled experiment to probe the mechanistic route and the key intermediate for the acetoxylation of **6a**; B) Electrostatic potential map of (i) iodine and (ii) acetyl hypoiodite at 0.001 electron bohr⁻³ isodensity surface highlighting the σ -hole region; C) Optimized structure and calculated interaction energy for (i) **6a**.Iodine complex and (ii) **6a**.acetyl hypoiodite complex. (M06-2X-D3/6-311G(d,p) for C,H; 6-311+G(d,p) for N,O; LANL08d basis set in conjunction with the LANL2DZ effective core potential (ECP) for I/IEFPCM(acetic acid))

The detection of hypoiodites in the reaction mixture is difficult due to its transient nature. However, Wei and coworkers were able to detect the iodite (IO_2^-) and hypoiodite ions (IO^-) with mass spectroscopy.^[26e] Pleasingly, we were also able to detect acetyl hypoiodite (m/z 186.10 [M^+]) with GC-MS in an 1:1:1 mixture of iodine, TBHP and acetic acid.^[17] Moreover, when the reaction was carried out with iodine (1 equiv) in the presence of silver acetate (AgOAc, 1 equiv) and in the absence of any oxidizing agent, the reaction was completed within 1.5 h and 65% of the acetoxylation product **16a** was obtained along with 30% of the ketone (Figure 5A, Equation (iii)). However, no product was formed when only AgOAc (1 equiv) was employed in the absence of iodine source (Equation (iv)). These controlled reactions confirmed the active hand of AcOI in the accomplishment of the reaction as AcOI is formed irreversibly in a 1:1 mixture of iodine and silver acetate in acetic acid.^[28] Finally, the reaction was carried with catalytic HI in absence and presence of TBHP (Equation (v) and Equation (vi)). No products were formed in the first case while 65% of acetoxylation products **16a** along with 25% of ketones **7a** were formed in the second case. These reactions indicated that if HI is generating in the reaction mixture it could not catalyze the reaction. The oxidation of HI to iodine (I) active species (acetyl hypoiodite) was mandatory for the completion of the reaction.

Further quantum chemical studies of electronic distribution on iodine and acetyl hypoiodite employing DFT showed that the size of the σ -hole (the electro-positive region through which the XB interaction takes place with Lewis bases) was higher in

acetyl hypoiodite than molecular iodine (Figure 5B). Hence, the interaction energy between 2-benzylpyridine and acetyl hypoiodite ($-33.0 \text{ kcal mol}^{-1}$) was higher than that of 2-benzylpyridine and molecular iodine ($-25.6 \text{ kcal mol}^{-1}$). The stronger XB interaction enabled the imine-enamine tautomerism more efficiently. Thus, the acetoxylation reaction was more efficient in iodine/TBHP/acetic acid system where acetyl hypoiodite is the key XB donor species than iodine/acetic acid system where iodine is the key XB donor species (Scheme 5d and 5b respectively).

The imine-enamine tautomerism of 2-benzylpyridine **6a** could also be enabled by the formation of hydrogen-bonded complex between **6a** and acetic acid. However, the calculation of change in free energy associated with two independent processes demonstrated that the formation of halogen-bonded adduct between **6a** and acetyl hypoiodite is more feasible ($\Delta G = -7.8 \text{ kcal mol}^{-1}$) than the formation of hydrogen-bonded adduct between **6a** and acetic acid ($\Delta G = -0.8 \text{ kcal mol}^{-1}$, Figure 6A). Thus, acetyl hypoiodite was the key intermediate which enabled the imine-enamine tautomerism of **6a**.

Finally, the halogen-bonding interaction between **6a** and acetyl hypoiodite was demonstrated using UV-vis spectroscopy and molecular modeling with time dependent DFT (TD-DFT) approach. A mixture of 1:1:1 iodine, TBHP and acetic acid was stirred for 0.5 h at 100 °C and the UV-vis absorption of the same was recorded in acetic acid at 10^{-4} (M) concentration.^[17] An absorption band appeared with the maxima at 474.9 nm for acetyl hypoiodite. However, when **6a** (1 equiv) was added to the same solution and the UV-vis spectra of the sample was recorded, the band at 474.9 nm completely disappeared and two new bands appeared with the maxima at 358.7 nm (blue-shifted band, λ_{BS}) and 291.3 nm (charge-transfer band, λ_{CT}) (Figure 6B).^[9b, 17, 32] The charge-transfer (CT) band merged with the broad absorption band of **6a** with the maxima at 270 nm. To overcome this problem, the UV-vis spectra of the same sample were recorded with a 10^{-4} (M) solution of **6a** in acetic acid as blank. The absorption band of **6a** was automatically cancelled out and the charge-transfer band with the maxima at 291.3 nm clearly emerged (Figure 6C).^[17]

The DFT calculation showed that the HOMO-LUMO gap of acetyl hypoiodite increased upon halogen-bonding complex formation with **6a** (from 6.59 eV to 7.10 eV, Figure 6D). This observation satisfactorily corroborated the observed blue shift in UV-vis experiment (from 474.9 nm to 358.7 nm). The TD-DFT calculation predicted the presence of one absorption maxima at 360.1 nm with low oscillator strength ($f = 0.0081$) and another absorption maxima with higher oscillator strength ($f = 0.0505$) than the previous one for the XB complex of CH_3COOI with **6a**. These results corroborated with the experimental values, i.e. 358.7 nm with low absorbance and 291.3 nm with higher absorbance.

Furthermore, this calculation revealed that 43.7% of the 292.4 nm absorption (CT band) was contributed by the excitation of electrons from HOMO-1 to LUMO+1 and 52.1% was contributed by the excitation of electrons from HOMO-1 to LUMO+2 (Figure 6E). These orbitals were largely located on the nitrogen of pyridine and the iodine atom of acetyl hypoiodite. Hence, the

TD-DFT simulation of the band at 291.3 nm clearly showed that this band appeared due to excitation of the electrons participating in the halogen-bonding interaction between the pyridine moieties of **6a** and the iodine of acetyl hypoiodite.

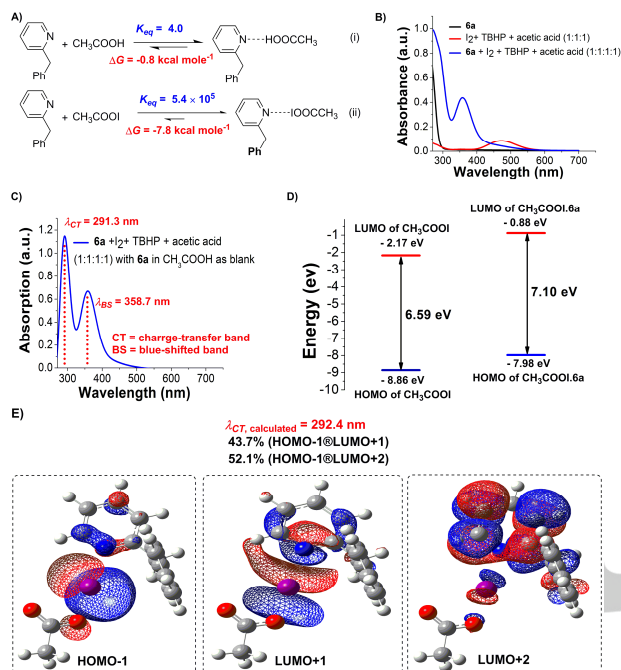


Figure 6. A) Calculation of free energy change for (i) HB adduct formation between **6a** and acetic acid (ii) XB adduct formation between **6a** and acetyl hypoiodite. B) UV-vis spectra of **6a**, $I_2 + TBHP + \text{acetic acid}$ (1:1:1) and **6a** + $I_2 + TBHP + \text{acetic acid}$ (1:1:1:1) in acetic acid (path length = 1 cm) at concentrations of 10^{-4} (M) for each species. C) UV-vis spectra of **6a** + $I_2 + TBHP + \text{acetic acid}$ (1:1:1:1) in acetic acid (path length = 1 cm) at concentrations of 10^{-4} (M) for each species keeping 10^{-4} (M) solution of **6a** in acetic acid as blank; D) Energy difference between the frontier orbitals of CH_3COOI (left) and of $CH_3COOI \cdot 6a$. E) TD-DFT simulation of UV-vis spectroscopic data of XB adduct of **6a** and acetyl hypoiodite.

Next, we tried to find out the key factor that controlled the selectivity of the acetoxylation over the ketone formation. For this, the reaction was carried out in several aliphatic organic acids with different pK_a values (Figure 7A). Neither acyloxylated product **17a** nor the ketone **7a** was observed when a stronger acid such as α -chloro acetic acid ($pK_a = 2.85$) was used as the solvent (entry 2, Figure 7A). It is worth mentioning that iodine remains in almost free molecular state (uncomplexed) in a strong and polar acidic medium whereas it forms a complex (XB complex) in weak acidic medium.^[33] These XB complexes are the pre-reactive species for the formation of acyl hypoiodites. The peroxide increases the electrophilicity of iodine by oxidizing it to iodine(I) and facilitates the formation of acyl hypoiodites. As the formation of pre-reactive complex is an elusive process in strong acid, it can be concluded that the required acyl hypoiodite intermediate couldn't be generated in α -chloro acetic acid and thus, no oxidative process was observed in this solvent.

Hence, we screened the straight and branched chain aliphatic acids having the pK_a values near the pK_a value of acetic acid ($pK_a = 4.76$). As a result, 60%, 53%, 45% and 43% yield of acyloxylated product was obtained in propanoic acid ($pK_a = 4.86$), butanoic acid ($pK_a = 4.83$), pentanoic acid ($pK_a = 4.83$) and 2-methylpropanoic acid ($pK_a = 4.88$) solvents respectively (entries 3–6, Figure 7A). Although, the reactions proceeded in all these solvents, the selectivity was lost and substantial amount of the ketone **7a** was isolated in the case of pentanoic acid and 2-methylpropanoic acid (entries 5 & 6, Figure 7A).

The preliminary experiments indicated that, a weak XB interaction could not enable the imine-enamine tautomerism of **6a** and thus the selectivity and efficiency of the reaction was less (Scheme 5 and Figure 5). Hence, initially it was intuited that the XB interactions between **6a** and acyl hypoiodites were reduced with the increase in the number of carbon in the aliphatic chain of acyl hypoiodites. The increasing +I effect of the aliphatic moiety of acyl hypoiodites could reduce the electrophilicity and the size of σ -hole of iodine atom.

However, to our surprise, a counter-intuitive result was obtained when we tried to compare the strength of XB interaction between the acyl hypoiodites and **6a** with DFT (Figure 7A and 7B). Gratifyingly, a thorough literature survey revealed that noncovalent interactions such as halogen bond often shows these kinds of uncommon trends.^[34] These counter-intuitive trends signify the charge-transfer character and substantial mixing of frontier orbitals (HOMO of donor and LUMO of acceptor) in a noncovalent adduct due to the presence of energetically low-lying LUMO on the acceptor moiety (here, XB donor).^[34c] In addition, according to Rosokha and coworkers, the mixing of frontier orbitals causes the lowering of the energy barrier for electron transfer (ET) from XB acceptor to XB donor.^[23b, 35] Hence, the energy of the HOMO of **6a** and the energy of the LUMOs of acyl hypoiodites were calculated with DFT to compare qualitatively the possibilities of mixing of LUMOs of the acyl hypoiodites with the HOMO of **6a** (Figure 7C).^[17]

Pleasingly, this analysis clearly showed that other acyl hypoiodites generated from propanoic acid, butanoic acid, pentanoic acid and 2-methylpropanoic acid had energetically low-lying LUMOs in comparison to the LUMO of acetyl hypoiodites (Figure 7C). Thus, the possibility of the ET process by orbital-mixing was increased in these solvent and was highest for pentanoic acid and 2-methylpropanoic acid (entry 5 & 6, Figure 7A). This selectivity study indicated that, a particular interaction energy between acyl hypoiodites and **6a** was required to maintain the selectivity of acyloxylation process. The weaker XB interaction could not enable the imine-enamine tautomerism and the stronger XB interaction increased the possibility of background ET process. In both the cases, the efficiency and the selectivity of the process were reduced. Furthermore, this selectivity study pointed out that role of halogen-bonding should be considered seriously during the designing and mechanistic analysis of halogen-based organocatalysis and the quantum chemical calculations can be a helpful means in this aspect.

A plausible mechanism for the iodine catalyzed acyloxylation reaction is designed based on the results of supporting experiments and quantum chemical calculations (Figure 7D). The acyl hypoiodite **18** is generated from the reaction of acid, TBHP and iodine. This acyl hypoiodite **18** undergoes feasible formation of XB adduct **19**. Although, the substrate **6a** can form the HB adduct **20** with solvent acid, the process is less thermodynamically favorable (Figure 6A). The intermediate **19** can be converted to the heterobenzyl iodide **22** by the means of imine–enamine tautomerism *via* intermediate **21**. The nucleophilic substitution of iodide with acid RCOOH at heterobenzyl position leads to the formation of acyloxylated

product **23**. The by-product HI can further be oxidized to **18** in the presence of TBHP. The ketone is generated by XB assisted ET from **6a** to **18** through the intermediacy of radical ion pair **19a** and heterobenzyl radical **15**.

The scope of the substrates was investigated to probe the efficiency of the process. The 2-benzylpyridines bearing electron-rich arenes provided acetylated product in good to excellent yields (**16b–16f**, Scheme 6). The methoxy group was well tolerated (**16b**). Moreover, the acetylation was not observed at other benzylic position when the starting materials that contain more than one benzylic position were subjected to the reaction conditions (**16c–16f**).

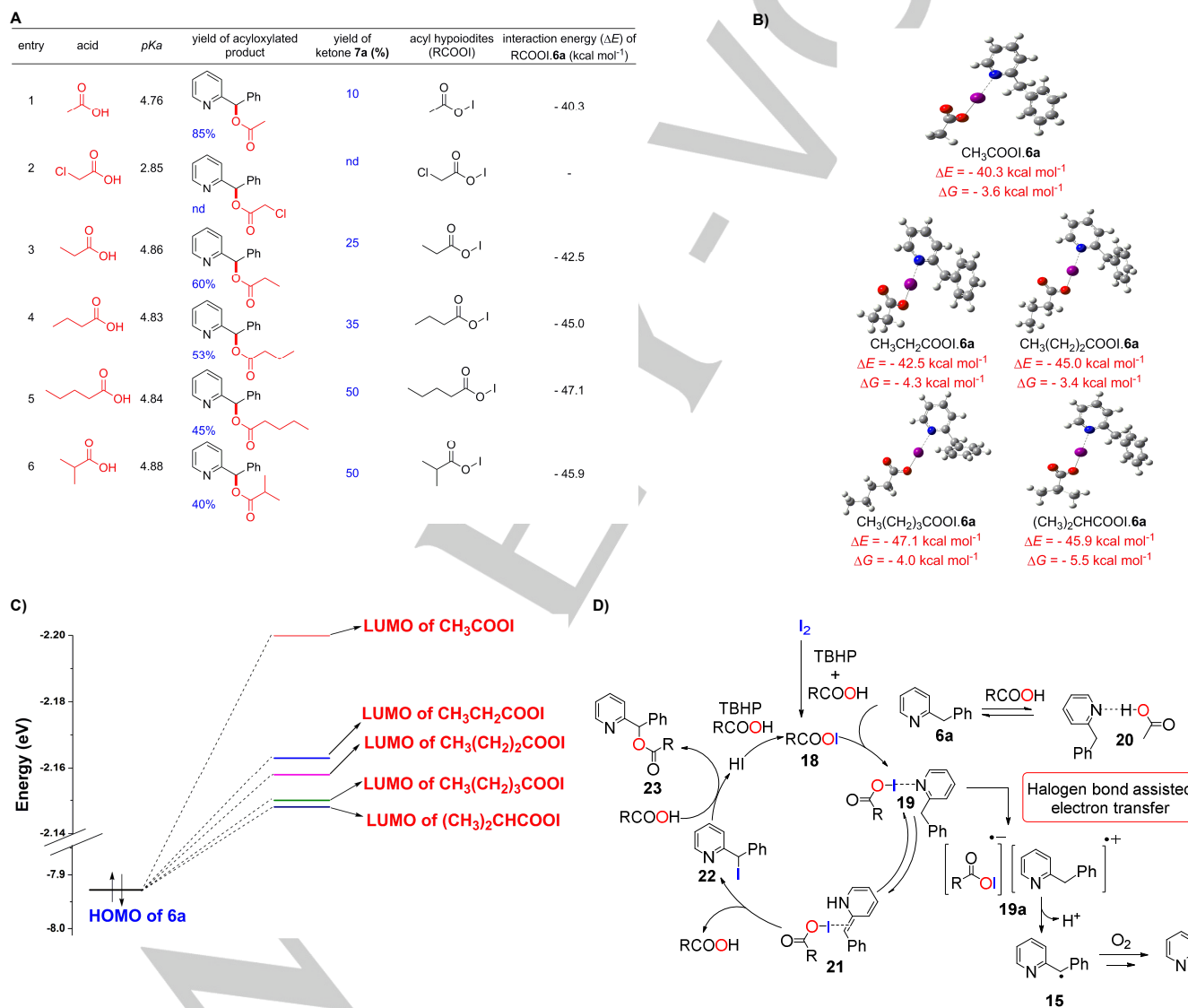
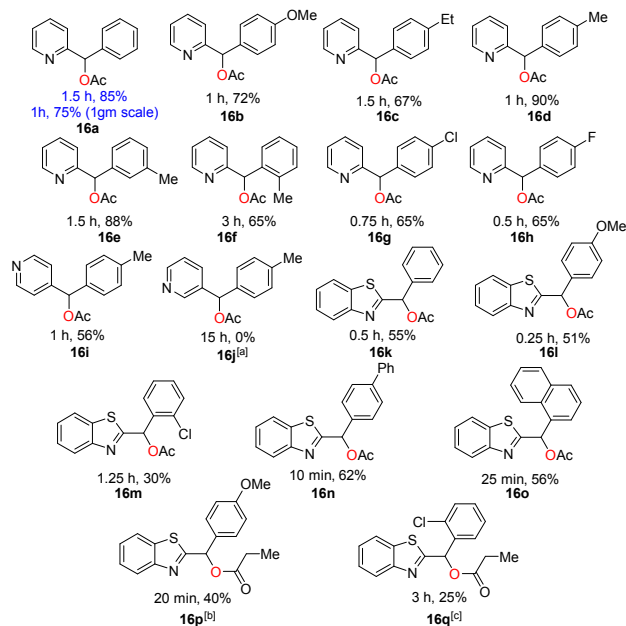


Figure 7. A) Selectivity study using different organic aliphatic acids with different pK_a s. B) Optimized structures of the acyl hypoiodites; (M06–2X–D3/6–311G(d,p) for C,H; 6–311+G(d,p) for N,O; LANL08d basis set in conjunction with the LANL2DZ effective core potential (ECP) for I) in vacuum; ΔE = BSSE corrected interaction energy; ΔG = free energy change of complexation. C) Frontier orbitals of the **6a** and acyl hypoiodites showing comparative possibilities of orbital mixing. The energies of the orbitals were calculated with DFT.^[17] D) Plausible reaction mechanism.



Scheme 7. Substrate scope for iodine catalysed acyloxylation reaction. In all the cases very trace amount of corresponding ketones have been formed. [a] Neither ketone nor acetylated product were isolated. [b] 30% corresponding ketone **7o** was isolated. [c] 25% corresponding ketone **7n** was isolated.

This observation highlighted the excellent chemo selectivity of this process where only the heterobenzylic position could be acetylated. The yield of the acetylated product was low in case of the substrate bearing 2-methyl arene (**16f**). This observation supported that the nucleophilic substitution at heterobenzylic position by acetic acid could be a crucial step in the mechanistic pathway.

The 2-benzylpyridines that contain electron withdrawing arenes provided moderate yields of the acetylated product and the reactions were very fast (**16g** and **16h**). The reaction was efficient for 4-benzylpyridine (**16i**) but did not work for 3-benzylpyridine (**16j**). This observation pointed out the importance of imine-enamine tautomerism during this acetylation process. Several benzothiazoles were also found to provide good yields of the acetylated products (**16k–16o**). The yield was low in the case of the benzothiazole bearing 2-substituted arene (**16m**). This observation further emphasized the possibility of nucleophilic substitution at heterobenzylic position by acetic acid. When the solvent was changed to propanoic acid, the yield of the acyloxyated product was reduced (**16p**, **16q**). Finally, the reaction was tried at 1 g scale and 75% yield of the acetylated product was obtained proving the scalability of the process (**16a**).

Conclusions

The selective oxidation of (aryl)(heteroaryl)methanes ($C(sp^3)-H$) to ketones ($C(sp^2)=O$) or esters ($C(sp^3)-O$) with metal-free halogen(I) catalysts is reported. The oxidation of (aryl)(heteroaryl)methanes to ketone has been designed with catalytic amount of NBS in DMSO. No external activator is required for imine-enamine tautomerism, as, NBS itself acts as the XB donor activator. Unlike the previous reports, Isotope-labeling experiments reveal that the solvent with nucleophilic oxygen atom can act as the source of oxygen. However, a background XB-assisted ET process is responsible for the generation of heterobenzylic radicals in the reaction mixture which can be quenched with molecular oxygen to generate the ketone too.

The acetylation reaction takes place in acetic acid in the presence of catalytic amount of iodine and stoichiometric amount of TBHP. The formation of acetyl hypoiodite is established with the help of several control experiments, GC-MS and UV-vis spectroscopy in combination with TD-DFT. The vital role of halogen bond in controlling the background ET process and maintaining selectivity of the reaction has been established for the first time. This result encourages the new possibilities of developing metal-free routes for oxidative functionalization of heterobenzylic C-H bond with other nucleophiles by avoiding the formation of ketone to access new medicinally and biologically important molecules.

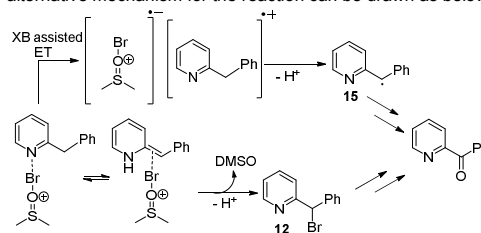
Acknowledgements ((optional))

We thank DST, New Delhi (SB/S1/OC-72/2013), and IIT Madras (CHY/17-18/847/RFIR/GSEK) for financial support.

Keywords: halogen bond • NBS catalyst • iodine catalyst • selective oxidation • (Aryl)(heteroaryl)-methanes

- [1] a) H. Zhang, K. Muñiz, *ACS Catal.* **2017**, *7*, 4122-4125; b) X. Wang, A. Studer, *Acc. Chem. Res.* **2017**, *50*, 1712-1724; c) S.-K. Wang, X. You, D.-Y. Zhao, N.-J. Mou, Q.-L. Luo, *Chem. Eur. J.* **2017**, *23*, 11757-11760; d) S. Wang, X. Zhang, C. Cao, C. Chen, C. Xi, *Green Chem.* **2017**, *19*, 4515-4519; e) S. Maksymenko, K. N. Parida, G. K. Pathe, A. A. More, Y. B. Lipisa, A. M. Szpilman, *Org. Lett.* **2017**, *19*, 6312-6315; f) T. Dohi, D. Koseki, K. Sumida, K. Okada, S. Mizuno, A. Kato, K. Morimoto, Y. Kita, *Adv. Synth. Catal.* **2017**, *359*, 3503-3508; g) G. L. Tolnai, U. J. Nilsson, B. Olofsson, *Angew. Chem. Int. Ed.* **2016**, *55*, 11226-11230; *Angew. Chem.* **2016**, *128*, 11392-11396 h) A. H. Sandtorv, D. R. Stuart, *Angew. Chem. Int. Ed.* **2016**, *55*, 15812-15815; *Angew. Chem.* **2016**, *128*, 16044-16047 i) I. Saikia, A. J. Borah, P. Phukan, *Chem. Rev.* **2016**, *116*, 6837-7042; j) F. Malmedy, T. Wirth, *Chem. Eur. J.* **2016**, *22*, 16072-16077; k) Y.-F. Liang, X. Li, X. Wang, M. Zou, C. Tang, Y. Liang, S. Song, N. Jiao, *J. Am. Chem. Soc.* **2016**, *138*, 12271-12277; l) M. S. Yusubov, V. V. Zhdkankin, *Resource-Efficient Technologies* **2015**, *1*, 49-67; m) C. Huo, M. Wu, F. Chen, X. Jia, Y. Yuan, H. Xie, *Chem. Commun.* **2015**, *51*, 4708-4711; n) M. Lamani, K. R. Prabhu, *Chem. Eur. J.* **2012**, *18*, 14638-14642; o) N. E. Leadbeater, M. Marco, *Angew. Chem. Int. Ed.* **2003**, *42*, 1407-1409; *Angew. Chem.* **2003**, *115*, 1445.

- [2] a) Y. Zhao, Y. Cotelte, N. Sakai, S. Matile, *J. Am. Chem. Soc.* **2016**, *138*, 4270-4277; b) G. Cavallo, P. Metrangolo, R. Milani, T. Pilati, A. Priimagi, G. Resnati, G. Terraneo, *Chem. Rev.* **2016**, *116*, 2478-2601; c) D. Bulfield, S. M. Huber, *Chem. Eur. J.* **2016**, *22*, 14434-14450; d) T. M. Beale, M. G. Chudzinski, M. G. Sarwar, M. S. Taylor, *Chem. Soc. Rev.* **2013**, *42*, 1667-1680.
- [3] a) D. von der Heiden, S. Bozkus, M. Klussmann, M. Breugst, *J. Org. Chem.* **2017**, *82*, 4037-4043; b) M. Saito, Y. Kobayashi, S. Tsuzuki, Y. Takemoto, *Angew. Chem. Int. Ed.* **2017**, *56*, 7653-7657; *Angew. Chem.* **2017**, *129*, 7761-7765 c) J.-P. Gliese, S. H. Jungbauer, S. M. Huber, *Chem. Commun.* **2017**, *53*, 12052-12055; d) A. Matsuzawa, S. Takeuchi, K. Sugita, *Chem. Asian J.* **2016**, *11*, 2863-2866; e) M. Breugst, E. Detmar, D. v. d. Heiden, *ACS Catal.* **2016**, *6*, 3203-3212; f) Y. Takeda, D. Hisakuni, C.-H. Lin, S. Minakata, *Org. Lett.* **2015**, *17*, 318-321; g) S. H. Jungbauer, S. M. Huber, *J. Am. Chem. Soc.* **2015**, *137*, 12110-12120; h) L. Zong, X. Ban, C. W. Kee, C.-H. Tan, *Angew. Chem. Int. Ed.* **2014**, *53*, 11849-11853; *Angew. Chem.* **2014**, *126*, 12043-12047 i) N. Tsuji, Y. Kobayashi, Y. Takemoto, *Chem. Commun.* **2014**, *50*, 13691-13694; j) W. He, Y.-C. Ge, C.-H. Tan, *Org. Lett.* **2014**, *16*, 3244-3247.
- [4] Y. Wang, J. Wang, G.-X. Li, G. He, G. Chen, *Org. Lett.* **2017**, 1442-1445.
- [5] S. Dordonne, B. Crousse, D. Bonnet-Delpont, J. Legros, *Chem. Commun.* **2011**, 47, 5855-5857.
- [6] F. Sladojevich, E. McNeill, J. Börgel, S.-L. Zheng, T. Ritter, *Angew. Chem. Int. Ed.* **2015**, *54*, 3712-3716; *Angew. Chem.* **2015**, *127*, 3783-3787
- [7] a) J. R. Khusnutdinova, D. Milstein, *Angew. Chem. Int. Ed.* **2015**, *54*, 12236-12273; *Angew. Chem.* **2015**, *127*, 12406-12445b) K. Fagnou, M. Lautens, *Angew. Chem. Int. Ed.* **2002**, *41*, 26-47; *Angew. Chem.* **2002**, *114*, 26-49. c) P. W. N. M. van Leeuwen, P. C. J. Kamer, J. N. H. Reek, P. Dierckx, *Chem. Rev.* **2000**, *100*, 2741-2770; d) D. J. Berrisford, C. Bolm, K. B. Sharpless, *Angew. Chem. Int. Ed.* **1995**, *34*, 1059-1070; *Angew. Chem.* **1995**, *107*, 1159. e) A. Padwa, D. J. Austin, *Angew. Chem. Int. Ed.* **1994**, *33*, 1797-1815; *Angew. Chem.* **1994**, *106*, 1881-1899.
- [8] I. Kazi, S. Guha, G. Sekar, *Org. Lett.* **2017**, *19*, 1244-1247.
- [9] a) S. Guha, I. Kazi, A. Nandy, G. Sekar, *Eur. J. Org. Chem.* **2017**, 2017, 5497-5518; b) S. Guha, I. Kazi, P. Mukherjee, G. Sekar, *Chem. Commun.* **2017**, 53, 10942-10945.
- [10] a) W. Jin, P. Zheng, W.-T. Wong, G.-L. Law, *Adv. Synth. Catal.* **2017**, *359*, 1588-1593; b) D. P. Hruszkewycz, K. C. Miles, O. R. Thiel, S. S. Stahl, *Chem. Sci.* **2017**, *8*, 1282-1287; c) H. Wang, Z. Wang, H. Huang, J. Tan, K. Xu, *Org. Lett.* **2016**, *18*, 5680-5683; d) H. Sterckx, J. De Houwer, C. Mensch, I. Caretti, K. A. Tehrani, W. A. Herrebout, S. Van Doorslaer, B. U. W. Maes, *Chem. Sci.* **2016**, *7*, 346-357; e) L. Ren, L. Wang, Y. Lv, G. Li, S. Gao, *Org. Lett.* **2015**, *17*, 2078-2081; f) J. Liu, X. Zhang, H. Yi, C. Liu, R. Liu, H. Zhang, K. Zhuo, A. Lei, *Angew. Chem. Int. Ed.* **2015**, *54*, 1261-1265; *Angew. Chem.* **2015**, *127*, 1277-1281. g) J. De Houwer, K. Abbaspour Tehrani, B. U. W. Maes, *Angew. Chem. Int. Ed.* **2012**, *51*, 2745-2748; *Angew. Chem.* **2012**, *124*, 2799-2802
- [11] a) B. Akhlaghinia, H. Ebrahimbadi, E. K. Goharshadi, S. Samiee, S. Rezazadeh, *J. Mol. Catal. A: Chem.* **2012**, *357*, 67-72; b) H. Jiang, H. Chen, A. Wang, X. Liu, *Chem. Commun.* **2010**, 46, 7259-7261; c) V. J. Traynelis, A. I. Gallagher, R. F. Martello, *J. Org. Chem.* **1961**, *26*, 4365-4368; d) V. J. Traynelis, R. F. Martello, *J. Am. Chem. Soc.* **1958**, *80*, 6590-6593; e) V. Boekelheide, W. J. Linn, *J. Am. Chem. Soc.* **1954**, *76*, 1286-1291.
- [12] A. Bruckmann, M. A. Pena, C. Bolm, *Synlett* **2008**, 2008, 900-902.
- [13] a) N. Kornblum, W. J. Jones, G. J. Anderson, *J. Am. Chem. Soc.* **1959**, *81*, 4113-4114; b) H. Nace, J. Monagle, *J. Org. Chem.* **1959**, *24*, 1792-1793.
- [14] a) E. Hu, N. Chen, M. P. Bourbeau, P. E. Harrington, K. Biswas, R. K. Kunz, K. L. Andrews, S. Chmait, X. Zhao, C. Davis, J. Ma, J. Shi, D. Lester-Zeiner, J. Danao, J. Able, M. Cueva, S. Talreja, T. Kornecook, H. Chen, A. Porter, R. Hungate, J. Treanor, J. R. Allen, *J. Med. Chem.* **2014**, *57*, 6632-6641; b) R. Shankar, S. S. More, M. V. Madhubabu, N. Vembu, U. K. Syam Kumar, *Synlett* **2012**, *23*, 1013-1020; c) J. Easmon, G. Heinisch, G. Pürstinger, T. Langer, J. K. Österreicher, H. H. Grunicke, J. Hofmann, *J. Med. Chem.* **1997**, *40*, 4420-4425; d) E. Frank, J. Gearien, M. Megahy, C. Pokorny, *J. Med. Chem.* **1971**, *14*, 551-553; e) A. Pelser, D. G. Müller, J. du Plessis, J. L. du Preez, C. Goosen, *Biopharm Drug Dispos.* **2002**, *23*, 239-244; f) N. A. Salvi, S. R. Udupa, A. Banerji, *Biotechnol. Lett.* **1998**, *20*, 201-203; g) V. Barouh, H. Dall, D. Patel, G. Hite, *J. Med. Chem.* **1971**, *14*, 834-836.
- [15] T. J. Ritchie, S. J. F. Macdonald, R. J. Young, S. D. Pickett, *Drug Discov Today* **2011**, *16*, 164-171.
- [16] E. Vitaku, D. T. Smith, J. T. Njardarson, *J. Med. Chem.* **2014**, *57*, 10257-10274.
- [17] See supporting information for details.
- [18] I. Castellote, M. Moron, C. Burgos, J. Alvarez-Builla, A. Martin, P. Gomez-Sal, J. J. Vaquero, *Chem. Commun.* **2007**, 1281-1283.
- [19] a) D. Brynn Hibbert, P. Thordarson, *Chem. Commun.* **2016**, *52*, 12792-12805; b) J. P. Wojciechowski, A. D. Martin, M. Bhadbhade, J. E. A. Webb, P. Thordarson, *CrystEngComm* **2016**, *18*, 4513-4517; c) P. Thordarson, *Chem. Soc. Rev.* **2011**, *40*, 1305-1323; d) *www.supramolecular.org*.
- [20] a) P. Zhangjin, F. Zhenwei, L. Beili, C. Jiajia, *Adv. Synth. Catal.* **2018**, *360*, 1761-1767; b) V. V. D., R. Edward, W. Eléna, M. Joseph, *Angew. Chem. Int. Ed.* **2017**, *56*, 3085-3089; *Angew. Chem.* **2017**, *129*, 3131-3135
- [21] P. K. Prasad, R. N. Reddi, A. Sudalai, *Org. Lett.* **2016**, *18*, 500-503.
- [22] The reaction mixture was injected into GC-MS during the course of reaction and no peak for bromodimethyl sulfoxonium ion was observed. This observation indicated that the bromodimethyl sulfonium ion did not generated in reaction mixture at 120 °C too. However, thermodynamically less stable bromodimethyl sulfonium ion can form in the reaction mixture via a kinetically controlled pathway and can react with **6a**. In this case, bromodimethyl sulfonium ion can form XB interaction with pyridine ring of **6a** and activate it and an alternative mechanism for the reaction can be drawn as below :



However, bromodimethyl sulfonium ions are transient at reaction temperature as the formation of bromodimethyl sulfonium ions follows a kinetically controlled pathway (K.C.P). Thus, very few molecules of **6a** can undergo this alternative route to generate intermediate **12** and **15** at reaction temperature.

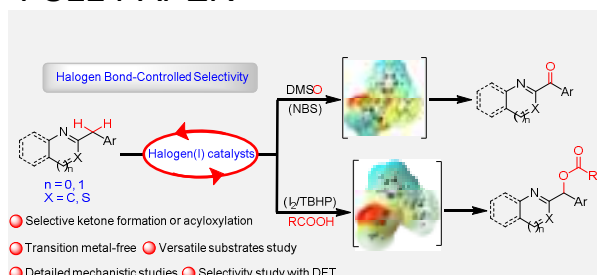
- [23] a) S. Rosokha, *Faraday Discuss.* **2017**, *203*, 315-332; b) S. V. Rosokha, M. K. Vinakos, *Phys. Chem. Chem. Phys.* **2014**, *16*, 1809-1813; c) S. V. Rosokha, J. K. Kochi, *Acc. Chem. Res.* **2008**, *41*, 641-653.
- [24] H. F. Askew, P. N. Gates, A. S. Muir, *J. Raman Spectrosc.* **1991**, *22*, 265-274.
- [25] a) M. Uyanik, K. Ishihara, *ChemCatChem* **2012**, *4*, 177-185; b) A. N. French, S. Bissmire, T. Wirth, *Chem. Soc. Rev.* **2004**, *33*, 354-362.
- [26] a) Y. Su, X. Zhou, C. He, W. Zhang, X. Ling, X. Xiao, *J. Org. Chem.* **2016**, *81*, 4981-4987; b) T. Froehr, C. P. Sindlinger, U. Kloeckner, P. Finkbeiner, B. J. Nachtsheim, *Org. Lett.* **2011**, *13*, 3754-3757; c) M. Uyanik, D. Suzuki, T. Yasui, K. Ishihara, *Angew. Chem. Int. Ed.* **2011**, *50*, 5331-5334; *Angew. Chem.* **2011**, *123*, 5443-5446 d) Y. Yan, Z.

- Wang, *Chem. Commun.* **2011**, 47, 9513-9515; e) C. Zhu, Y. Wei, *ChemSusChem* **2011**, 4, 1082-1086; f) M. Uyanik, H. Okamoto, T. Yasui, K. Ishihara, *Science* **2010**, 328, 1376-1379.
- [27] E. T. Urbansky, B. T. Cooper, D. W. Margerum, *Inorg. Chem.* **1997**, 36, 1338-1344.
- [28] R. B. Woodward, F. V. Brutcher, *J. Am. Chem. Soc.* **1958**, 80, 209-211.
- [29] Y. Ogata, I. Urasaki, *J. Chem. Soc. C* **1970**, 1689-1691.
- [30] R. C. Cambie, D. Chambers, P. S. Rutledge, P. D. Woodgate, *J. Chem. Soc., Perkin Trans. 1* **1978**, 1483-1485.
- [31] T. R. Beebe, B. A. Barnes, K. A. Bender, A. D. Halbert, R. D. Miller, M. L. Ramsay, M. W. Ridenour, *J. Org. Chem.* **1975**, 40, 1992-1994.
- [32] C. Reid, R. S. Mulliken, *J. Am. Chem. Soc.* **1954**, 76, 3869-3874.
- [33] R. E. Buckles, J. F. Mills, *J. Am. Chem. Soc.* **1953**, 75, 552-555.
- [34] a) W. Zierkiewicz, M. Michalczyk, *Theor. Chem. Acc.* **2017**, 136, 125; b) S. M. Huber, E. Jimenez-Izal, J. M. Ugalde, I. Infante, *Chem. Commun.* **2012**, 48, 7708-7710; c) F. Bessac, G. Frenking, *Inorg. Chem.* **2003**, 42, 7990-7994.
- [35] S. V. Rosokha, C. L. Stern, J. T. Ritzert, *Chem. Eur. J.* **2013**, 19, 8774-8788.

Entry for the Table of Contents (Please choose one layout)

Layout 2:

FULL PAPER



Interaction matters: The role of halogen–bonding interaction in the selective oxidation of (Aryl)(heteroaryl)-methanes to Ketones or Esters with Bromine(I) and Iodine(I) catalysts, respectively, has been thoroughly demonstrated.

Somraj Guha, Govindasamy Sekar*

Page No. – Page No.

Metal-free Halogen(I) Catalysts for Oxidation of (Aryl)(heteroaryl)-methanes to Ketones or Esters : Selectivity Control by Halogen Bond

Accepted Manuscript